Journal of Computing and Electronic Information Management
ISSN: 2413-1660 | Vol. 19, No. 3, 2025

Dynamic Simulation of Flywheel Energy Storage Beam Pumping Unit System and Adaptive Frequency Conversion Voltage Regulation Energy-Saving Optimization

Jingyi Wu, Shenghu Pan

School of Mechanical Engineering, Southwest Petroleum University, Chengdu 610500, China

Abstract: Installing a flywheel energy storage device in a beam pumping unit can effectively suppress fluctuations in the motor speed and output power of the pumping unit, reduce its peak power, improve efficiency, and lower the installed power capacity. However, while influencing the motor speed, the flywheel energy storage device indirectly affects the motion law and loading conditions of the pumping unit, and its impact varies with different equipment models. This renders the original pumping unit stroke frequency controller inadequate for the new system. By analyzing the motion and load characteristics of the pumping unit, this paper proposes an adaptive frequency conversion and voltage regulation control technology based on fuzzy PID and frequency converters. This technology alters the operating state of the pumping unit by adjusting the motor frequency. Its main features include: 1) Deriving an optimized frequency curve under constant stroke frequency conditions using a pumping unit frequency conversion optimization algorithm. 2) Indirectly modifying the acceleration at the polished rod to reduce dynamic loads through frequency conversion. 3) Utilizing the adaptive adjustment capability of fuzzy PID to eliminate the delay effect of the flywheel energy storage device on motor speed changes. A theoretical and simulation analysis was conducted using a CYJ10 model pumping unit and a flywheel energy storage system with a moment of inertia of 5 kg·m² as a case study. The energy-saving control effect was compared through simulation and measurement. The results indicate that the established simulation model has high accuracy and is referential. Adaptive frequency optimization control can significantly improve the dynamic performance of the new pumping unit system, notably reducing the polished rod load, increasing the motor load factor, decreasing the average power consumption, resulting in an overall system energy saving rate of 12%.

Keywords: Flywheel energy storage; Constant voltage-frequency ratio; Fuzzy PID; Beam pumping unit; Three-phase asynchronous motor.

1. Introduction

Beam pumping units, widely utilized in the oil extraction industry, represent a critical component for mechanical oil recovery, accounting for a significant portion of energy consumption in oilfields due to their intermittent load characteristics and torque fluctuations [1]. Traditional systems often suffer from inefficiencies, such as negative torque in gearboxes and high energy losses during upstroke and downstroke cycles, prompting the need for advanced energy-saving technologies [2]. Flywheel energy storage systems (FESS) have emerged as a promising solution to mitigate these issues by storing kinetic energy during low-load phases and releasing it during high-demand periods, thereby balancing the motor load and enhancing overall system efficiency [3]. Dynamic simulation plays a pivotal role in analyzing and optimizing such integrated systems, allowing for the evaluation of mechanical and electrical behaviors under varying operational conditions [4]. Previous studies have demonstrated the effectiveness of flywheel integration in beam pumping units through simulation models that capture energy absorption and release mechanisms, showing potential reductions in peak power demands and improved stability [5]. However, standalone flywheel approaches may not fully address voltage and frequency variations that contribute to energy wastage in asynchronous motors commonly used in these units [6].To further enhance energy savings, adaptive frequency conversion and voltage regulation techniques have been explored, enabling real-time adjustments based on load profiles to minimize power consumption while maintaining operational performance [7]. Sectional control strategies that combine variable frequency (VF) and voltage regulation (VR) have shown superior results in beam pumping motor systems (BPMS), adapting to the cyclical nature of strokes for optimized energy use [8]. Intelligent optimization methods, such as those based on deep reinforcement learning, have also been proposed to fine-tune frequency modulation, achieving adaptive responses to dynamic field conditions [9].This study focuses on the dynamic simulation of a hybrid flywheel energy storage beam pumping unit system coupled with adaptive frequency conversion voltage regulation for energy-saving optimization. By integrating these technologies, the proposed approach aims to simulate system dynamics, evaluate energy efficiency gains, and develop an adaptive control framework that responds to real-time operational parameters, ultimately contributing to sustainable oil production practices [10].

2. Analysis of Geometric Motion Characteristics of Pumping Unit Four-Bar Linkage

The schematic diagram of the four-bar linkage structure of a beam pumping unit is shown in Figure 2.1. Here, A is the length of the front arm of the walking beam (m), P is the length of the connecting rod (m), R is the crank radius (m), C is the length of the rear arm of the walking beam (m), β is the

angle between the connecting rod and the walking beam (°), θ_2, θ_3, θ_4 are the angular displacements (°) of the crank, connecting rod, and walking beam relative to the line connecting the crank rotation center and the walking beam rotation center, respectively; $\dot{\theta}_2$, $\dot{\theta}_3$, $\dot{\theta}_4$ are the first derivatives of the corresponding angular displacements, i.e., angular velocities (rad/s).

Derived from the systems geometric relationships, θ_3, θ_4 are:

$$\begin{cases} \dot{\theta}_3 = \dfrac{R\dot{\theta}_2}{P}\dfrac{sin(\theta_4-\theta_2)}{sin(\theta_3-\theta_4)} \\ \dot{\theta}_4 = \dfrac{R\dot{\theta}_2}{C}\dfrac{sin(\theta_3-\theta_2)}{sin(\theta_3-\theta_4)} \end{cases} \quad (1)$$

Differentiating $\dot{\theta}_3$, $\dot{\theta}_4$ yields the corresponding angular accelerations $\ddot{\theta}_3$, $\ddot{\theta}_4$:

$$\begin{cases} \ddot{\theta}_3 = \dot{\theta}_3\left[\dfrac{\ddot{\theta}_2}{\dot{\theta}_2} + (\dot{\theta}_4-\dot{\theta}_2)\cot(\theta_4-\theta_2) - (\dot{\theta}_3-\dot{\theta}_4)\cot(\theta_3-\theta_4)\right] \\ \ddot{\theta}_4 = \dot{\theta}_4\left[\dfrac{\ddot{\theta}_2}{\dot{\theta}_2} + (\dot{\theta}_2-\dot{\theta}_3)\cot(\theta_2-\theta_3) - (\dot{\theta}_3-\dot{\theta}_4)\cot(\theta_3-\theta_4)\right] \end{cases} \quad (2)$$

Since within a single cycle, for any crank angular displacement θ_2, both θ_3 and θ_4 are uniquely determined, and are independent of $\dot{\theta}_2$ and $\ddot{\theta}_2$, then θ_3, θ_4, $\dot{\theta}_3$, $\dot{\theta}_4$ can all be expressed as functions of $\dot{\theta}_2$ and $\ddot{\theta}_2$. Introducing parameters D_1–D_4, the equation system is as follows:

$$\begin{cases} D_1 = \dfrac{R}{P}\dfrac{\sin(\theta_4-\theta_2)}{\sin(\theta_3-\theta_4)} \\ D_2 = \dfrac{R}{C}\dfrac{\sin(\theta_3-\theta_2)}{\sin(\theta_3-\theta_4)} \\ D_3 = \dfrac{R}{C}\dfrac{\cos(\theta_2-\theta_3)}{\sin(\theta_3-\theta_4)} \\ D_4 = \cot(\theta_3-\theta_4) \end{cases} \quad (3)$$

Substituting equation system (3) into systems (1) and (2) yields:

$$\begin{cases} \dot{\theta}_3 = \dot{\theta}_2 \cdot D_1 \\ \dot{\theta}_4 = \dot{\theta}_2 \cdot D_2 \\ \ddot{\theta}_4 = D_2\left[\ddot{\theta}_2 - (D_1-D_2)D_4\dot{\theta}_2^{\,2}\right] - D_3(1-D_1)\dot{\theta}_2^{\,2} \end{cases} \quad (4)$$

The polished rod velocity v and acceleration a are respectively:

$$v = A\cdot\dot{\theta}_4 = \frac{AR}{C}\frac{\sin(\theta_3-\theta_2)}{\sin(\theta_3-\theta_4)}\dot{\theta}_2 \quad (5)$$

$$a = A\cdot\ddot{\theta}_4 = A\cdot\left\{D_2\left[\ddot{\theta}_2 - (D_1-D_2)D_4\dot{\theta}_2^{\,2}\right] - D_3(1-D_1)\dot{\theta}_2^{\,2}\right\} \quad (6)$$

According to equation (6), the magnitude of the polished rod acceleration a is mainly related to the magnitude of $\dot{\theta}_2$ and $\ddot{\theta}_2$. Since the time for a single cycle of the pumping unit is greater than 6 seconds, the crank basically rotates at a stable speed, and the absolute value of the crank angular acceleration is small, the influence of angular acceleration on the polished rod acceleration can be ignored to simplify the mathematical model. Introducing parameter $D_5 = -D_2 D_4 (D_1 - D_2) - D_3 (1 - D_1)$ yields:

$$a = A\cdot\ddot{\theta}_4 = A\cdot D_5\cdot\dot{\theta}_2^{\,2} \quad (7)$$

Since the variation law of D_5 is only related to the geometric structure and position of the pumping unit, for any determined $\dot{\theta}_2$, D_5 has a uniquely corresponding value, independent of the crank angular velocity $\dot{\theta}_2$. Therefore, the polished rod acceleration a at any moment within a single cycle is proportional to the square of the crank angular velocity, $\dot{\theta}_2^{\,2}$.

The relationship between the crank angular velocity $\dot{\theta}_2$ and the motor angular velocity ω is:

$$\dot{\theta}_2 = \frac{\omega}{k} \quad (8)$$

where k is the gear ratio of the reduction gearbox. Also, since:

$$\omega = \frac{2\pi n}{60} \quad (9)$$

where n is the motor speed (rpm). The relationship between crank angular velocity and motor speed is:

$$\dot{\theta}_2 = \frac{2\pi n}{60k} \quad (10)$$

The relationship between motor speed n, frequency f, and pole pair number p is: $n = 60f / p$. Thus, controlling the motor frequency can control the motor speed. The relationship between frequency f, speed n, rated frequency f_0, and rated speed n_0 is:

$$\frac{f}{n} = \frac{f_0}{n_0} = \frac{60}{p} \quad (11)$$

Combining equations (10) and (11) yields:

$$\dot{\theta}_2 = \frac{2\pi f}{k\cdot p} \quad (12)$$

From equation (12), there is a positive correlation between motor frequency and crank angular velocity. From equations (12) and (7), the relationship between frequency f and polished rod acceleration a is:

$$f = \sqrt{\frac{a}{A\cdot D_5}}\cdot\frac{60k}{2\pi}\cdot\frac{f_0}{n_0} \quad (13)$$

In equation 13, except for f, a, and D_5, all other quantities are constants, and D_5 is only related to the crank displacement θ_2, independent of f and a. Clearly, the frequency f is proportional to the square root of the polished rod acceleration, $\sqrt{a}$. Thus, it can be concluded that the magnitude of the polished rod acceleration a can be altered by controlling the motor frequency f.

3. Analysis of Pumping Unit Crank Torque Characteristics

From the mechanical dynamics theory of the pumping unit, the crank motion equation is obtained:

$$\begin{cases} M_{ed} - M_{ef} = J_e\ddot{\theta}_2 + \dfrac{1}{2}\dot{\theta}_2\dfrac{dJ_e}{d\theta_2} \\ M_{ef} = (P_L - B_W)\cdot T_f - M_c\cdot sin(\theta-\tau) \end{cases} \quad (14)$$

where, M_{ed} is the net crank torque; M_{ef} is the load torque; J_e is the equivalent moment of inertia of all moving parts of the pumping unit converted to the crank; P_L is the polished rod load; B_W is the structural counterbalance weight; T_f is the torque factor; M_c is the maximum counterbalance torque of the counterweight; τ is the counterweight offset angle.

Since the speed ratios of the moving parts of the four-bar linkage can be expressed as functions of the crank angular displacement θ_2, the equivalent moment of inertia of the walking beam varies with the crank position. According to mechanical dynamics theory, the equivalent moment of inertia generates inertial torque due to angular acceleration and its own variation. Therefore, based on the solution equation for the load torque M_{ef}, when the pumping unit parameters are fixed, the load torque M_{ef} is only related to the polished rod load PL. The relationship is shown in Figure (). It can be observed that optimizing the polished rod load P_L optimizes the net crank torque at the dead points of the upstroke and downstroke, thereby reducing the motors output power and achieving energy savings.

4. Analysis of Pumping Unit Load and Polished Rod Load

The polished rod load of a beam pumping unit includes static loads and dynamic loads. Static loads consist of the weight of the sucker rods Prod, the weight of the oil column on the plunger inside the tubing Poil, and the pressure on the lower end of the plunger from the oil column outside the tubing Ppressure. Static loads are inherent to the pumping unit and depend only on the unit itself and downhole conditions. For deep well operations or pumping units with high stroke frequencies, the influence of dynamic loads must be considered. The dynamic loads of the pumping unit mainly consist of inertial loads and vibrational loads. Since downhole conditions significantly affect vibrational loads, making quantitative analysis difficult, this paper only analyzes inertial loads for simplicity. The inertial load Pg includes two parts: the sucker rod string inertial load $P_{oil\_inertia}$ and the oil column inertial load $P_{oil\_inertia}$. If elastic effects are neglected, the motion law of each point on the sucker rod string and oil column can be considered identical to that of the polished rod. Therefore, the magnitudes of $P_{oil\_inertia}$ and $P_{oil\_inertia}$ are proportional to the magnitude of the polished rod acceleration a, acting in the opposite direction to the acceleration.

The relationship between the load torque Mef and the polished rod load PL is illustrated in Fig. 1, which shows the variation of net crank torque at the upstroke and downstroke dead points under different control strategies.

Furthermore, Fig. 2 compares the crank torque characteristics with and without adaptive control. These results confirm that polished rod load optimization, combined with flywheel inertia and frequency adjustment, plays a critical role in enhancing system efficiency.

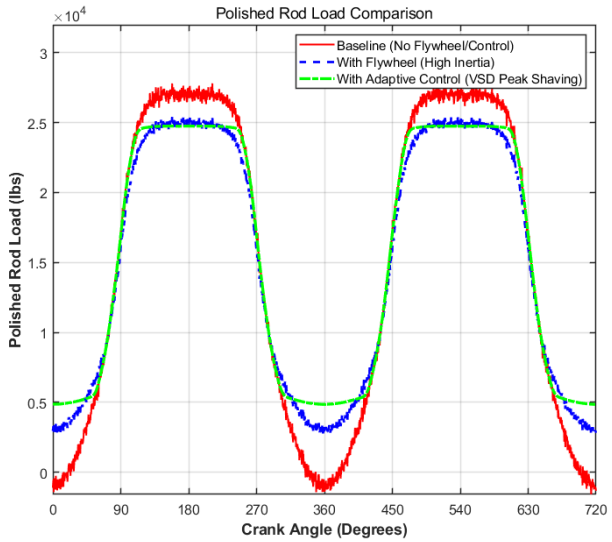

Fig. 1 Variation of net crank torque at upstroke and downstroke dead points with polished rod load optimization.

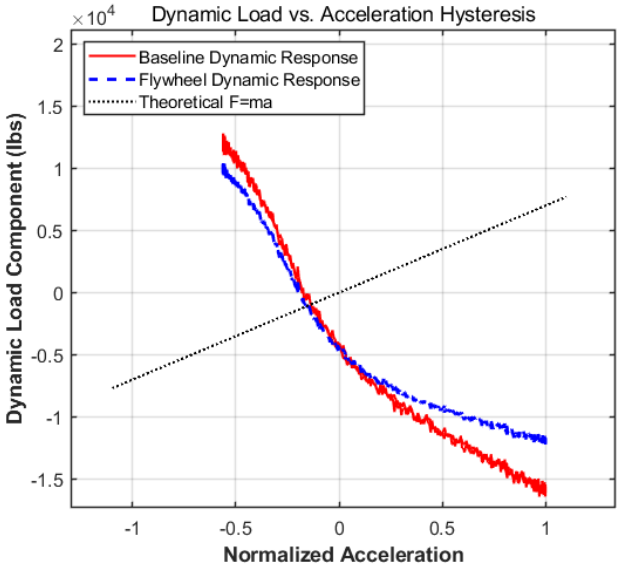

Fig. 2 Crank torque characteristics. (a) Without optimization. (b) With adaptive control.

5. Summary

This paper investigates the integration of a flywheel energy storage system (FESS) with a beam pumping unit to address inefficiencies in oil extraction, such as motor speed fluctuations, high peak power, and energy losses. By analyzing the geometric motion characteristics of the four-bar linkage mechanism, crank torque, and polished rod loads, the study demonstrates that polished rod acceleration is proportional to the square of the crank angular velocity, which can be controlled via motor frequency adjustments. An adaptive frequency conversion and voltage regulation control strategy, based on fuzzy PID and constant voltage-frequency ratio, is proposed to optimize system performance. This approach derives an optimized frequency curve, reduces dynamic loads by modifying polished rod acceleration, and mitigates delays from the flywheel on motor speed changes.

Using a CYJ10 beam pumping unit model with a flywheel moment of inertia of 5 kg·m² as a case study, dynamic simulations and theoretical analyses were conducted. Results show that the proposed method significantly improves dynamic performance, reduces polished rod loads, increases motor load factor, and lowers average power consumption, achieving an overall energy-saving rate of 12%. The simulation model exhibits high accuracy, providing a reference for enhancing sustainability in oil production through hybrid energy storage and intelligent control technologies. Future work could extend this to incorporate vibrational loads and real-world field validations.

References

[1] Yang, H., Wang, J., & Liu, H. (2021). Energy-saving mechanism research on beam-pumping unit driven by hydraulics. PLoS ONE, 16(4), Article e0249244.

[2] Xu, J., et al. (2024). Kinematic and dynamic analysis of eccentric balanced positive torque pumping unit. Machines, 12(4), 240.

[3] Xu, K., Guo, Y., Lei, G., & Zhu, J. (2023). A review of flywheel energy storage system technologies. Energies, 16(18), Article 6462.

[4] Muljadi, E., & Gevorgian, V. (2017). Flywheel energy storage - Dynamic modeling [Paper]. 9th Annual IEEE Green

Technologies Conference, Green Tech 2017, Denver, United States.

[5] Han, C., Tian, D., & Zhou, Y. (2020). Simulation analysis of flywheel energy storage beam pumping unit. Energy Storage Science and Technology, 9(4), 1186-1192.

[6] Zhou, Y., Chen, X., Jian, L., Wang, F., Tian, D., & Han, C. (2022). Design and experimental research on flywheel energy storage system of beam pumping unit. Energy Storage Science and Technology, 11(2), 593-599.

[7] Wang, Y., Eldeeb, H. H., Zhao, H., & Mohammed, O. A. (2019). Sectional variable frequency and voltage regulation control strategy for energy saving in beam pumping motor systems. IEEE Access, 7, 92456–92464.

[8] Wang, Y., Eldeeb, H. H., Zhao, H., & Mohammed, O. A. (2019). Sectional variable frequency and voltage regulation control strategy for energy saving in beam pumping motor systems. IEEE Access, 7, 92456–92464.

[9] Zhang, R., Chen, D., & Xiao, L. (2023). Intelligent method to optimize the frequency modulation for beam pumping system based on deep reinforcement learning. ACS Omega, 8(10), 9475–9485.

[10] Gao, Z.-W., & Jia, S. (2024). Modeling and control for beam pumping units: An overview. Processes, 12(7), Article 1468.